Development 130, 763-774

doi:10.1242/dev.00304

The tumor-suppressor and cell adhesion molecule Fat controls planar polarity via physical interactions with Atrophin, a transcriptional co-repressor

Manolis Fanto[1], Lesley Clayton[1], Jamie Meredith[1], Kirsten Hardiman[1], Bernard Charroux[2], Stephen Kerridge[2] and Helen McNeill[1,*]

[1]Cancer Research UK (ICRF), London Research Institute, 44 Lincoln's Inn Fields, London WC2A 3PX, UK
[2]Laboratoire de Génétique et Physiologie du Développement, CNRS-INSERM-Université de la Méditerranée-AP de Marseille, Campus de Luminy Case 907, F-13288 Marseille, Cedex 09, France
*Author for correspondence (e-mail: helen.mcneill@cancer.org.uk)

Accepted 7 November 2002

SUMMARY

Fat is an atypical cadherin that controls both cell growth and planar polarity. Atrophin is a nuclear co-repressor that is also essential for planar polarity; however, it is not known what genes Atrophin controls in planar polarity, or how Atrophin activity is regulated during the establishment of planar polarity. We show that Atrophin binds to the cytoplasmic domain of Fat and that Atrophin mutants show strong genetic interactions with *fat*. We find that both *Atrophin* and *fat* clones in the eye have non-autonomous disruptions in planar polarity that are restricted to the polar border of clones and that there is rescue of planar polarity defects on the equatorial border of these clones. Both *fat* and *Atrophin* are required to control *four-jointed* expression. In addition our mosaic analysis demonstrates an enhanced requirement for *Atrophin* in the R3 photoreceptor. These data lead us to a model in which *fat* and *Atrophin* act twice in the determination of planar polarity in the eye: first in setting up positional information through the production of a planar polarity diffusible signal, and later in R3 fate determination.

Key words: Planar polarity, Adhesion, *Drosophila*, Eye, Atrophin, Fat

INTRODUCTION

Polarity is a fundamental characteristic of most cells and is essential for their proper function. Cellular polarity has been intensively investigated, and significant progress has been made in revealing the mechanisms that underlie the establishment of cellular polarity. Another widespread, but less understood, form of polarity is planar polarity (PP), which is the organization of cells within the plane of the epithelium. Intensive recent investigations have demonstrated that a conserved PP pathway works to coordinate the polarity of adjacent cells in such divergent systems as convergent extension movements in zebrafish and frogs, and the polarity of wing hairs in the fly (Axelrod and McNeill, 2002).

Studies primarily in the fly have implicated a Frizzled (Fz) signaling pathway as being central to the control of PP (Adler and Lee, 2001). Analysis of clones of *fz* mutant cells reveals both cell autonomous and non-autonomous defects in PP. This has led to the suggestion that Fz, a seven-pass transmembrane receptor (Adler et al., 1990; Park et al., 1994) is involved in both the reception of a PP signal and in its transmission to adjacent cells. Recent work has demonstrated that Fz is part of an asymmetrically localized signaling complex, which also contains the signaling protein Dishevelled and the atypical cadherin, Flamingo (Axelrod, 2001; Das et al., 2002; Strutt et al., 2002; Strutt, 2001; Tree et al., 2002; Usui et al., 1999). How Fz signaling activity is controlled is not clear.

A well-studied system for understanding the control of PP is the fly eye (Wolff and Ready, 1993). The fly eye is composed of ~800 photoreceptor clusters called ommatidia, each composed of eight photoreceptors, R1-R8, as well as a number of accessory cells (Fig. 1A). Ommatidia are organized into dorsal and ventral fields of mirror-image planar polarity, which meet at the equator (Fig. 1A,C). PP develops in the eye imaginal disc shortly after ommatidial preclusters assemble. Preclusters in the dorsal and ventral fields rotate 90° in opposite directions away from the equator, producing mirror image fields. Genetic studies have suggested that *fz* is necessary for interpreting and communicating a PP signal that is thought to emanate from the equator. *fz* has also been implicated in controlling R3 cell fate (Zheng et al., 1995). Intensive work has suggested that photoreceptors R3 and R4 are crucial in directing the rotation of preclusters. In addition it has been shown that the member of the R3/R4 pair with higher Notch activity will take on the R4 fate. This decision directs precluster rotation (Cooper and Bray, 1999; Fanto and Mlodzik, 1999; Tomlinson and Struhl, 1999).

The atypical cadherins Fat (Ft) and Dachsous (Ds) act upstream of *fz*, and may control Fz activity during the development of PP. Two separate models have been proposed to explain how Fat and Ds control planar polarity in the eye.

In one model, Fat controls Fz activity, and biases the equatorially localized cell to an R3 fate (Yang et al., 2002). In another model, *ft* inhibits equator formation, and this inhibition is relieved, through an unknown mechanism, at the presumptive equator (Rawls et al., 2002).

We have isolated several new *ft* alleles in a screen to identify genes involved in cell adhesion and planar polarity in the eye (Fig. 1B). To understand how *ft* functions in PP, we conducted a yeast two-hybrid screen to identify proteins that bind the cytoplasmic domain of Fat. One protein identified by this screen was *Drosophila* Atrophin (Atro; also known as Grunge), which is the sole *Drosophila* homolog of human Atrophins (Erkner et al., 2002; Zhang et al., 2002). Mutations in Atrophin 1 cause dentatorubal-pallidoluysian atrophy (DRPLA) (Koide et al., 1994; Nagafuchi et al., 1994), a progressive neurodegenerative disease associated with ataxia, epilepsy, myoclonus and choreoathetosis. Atro is a nuclear protein that has been recently shown to act as a transcriptional co-repressor with roles in segmentation and dorsoventral patterning. Significantly, Atro has also been shown to control PP in the eye and the wing (Zhang et al., 2002).

We show here that Fat and Atro physically interact, display strong genetic interactions, and control similar processes in development. Our analysis of *ft* and *Atro* clones in the eye reveals alterations in planar polarity at the polar border of the clone as well as equatorial rescue of mutant tissue. In addition, our mosaic analysis of these clones demonstrates that both *ft* and *Atro* are needed specifically in the R3 cell. We also show that *Atro* (like *ft*) controls expression of *four-jointed* (*fj*), a gene that can control PP. These data lead us to propose that *ft* and *Atro* act at least twice in the development of PP; initially to control PP gradients and later in R3 fate decisions.

MATERIALS AND METHODS

Yeast two-hybrid screen

Bait 1 derives from a cDNA of the cytoplasmic region of *ft* (Research Genetics) cut with *Nco*I and *Bsr*BI (nucleotides 14760 to 15209) and ligated in frame with the GAL4 DNA binding domain into pAS2-1 (Clontech). Bait 2 was generated from a non-overlapping region of the cytoplasmic domain of *ft* by PCR amplification (nucleotides 13879 to 14505). Baits were confirmed by sequencing. Bait plasmids were co-transformed into AH109 yeast with a *Drosophila* embryonic cDNA library in the pACT2 vector (Clontech) using the standard Lithium Acetate transformation. Interactors were selected on SD media lacking Ura, Trp, His, Leu and Ade and tested for activation of the reporter gene using X-gal filter assays (Clontech). pACT2 plasmids were extracted, inserts were PCR amplified and sequenced. Approximately 10^5 clones were screened for each bait. Interactors were re-tested against pAS2-1 containing bait protein and against the empty pAS2-1 vector to check for autoactivation of the reporter genes.

Fly stocks and genetics

For the screen, male *w; 40FRT* flies were mutagenized with ethyl methyl sulphonate using standard procedures. These flies were crossed to females *hsFlp,w; 40FRT*, their progeny heat-shocked to induce clones and then screened for clones that had smooth edges. Mitotic clones were generated by the Flp/FRT technique with either hsFlp or eyFlp and marked in imaginal discs by Ubi-GFP (Rawls et al., 2002; Yang et al., 2002). Mutant alleles used were ft^{GRV}, ft^{fd}, ft^{1},ds^{UAO71}, $Atro^{11}$, $Atro^{35}$, $Atro^{i5A3}$ and *mδ0.5-lacZ* (described in FlyBase), *UAS-Atro* flies were a gift from Tian Xu. ft^{alb} and ft^{so} were obtained in our clone shape screen and shown to be *ft* alleles by complementation analysis. ft^{chance} was generated by imprecise excision of an adjacent P element (H. M., unpublished).

Immunohistochemistry and histology

Third instar imaginal discs were fixed in PLP (Fanto and Mlodzik, 1999). Primary antibodies were used as follows: rabbit anti-Atro (Erkner et al., 2002) (1:100), rat anti-Elav (DHSB, 1:1000), mouse anti-β-Gal (Promega 1:1000), rabbit anti-Bar (gift from Dr Saigo, 1:1000) and mouse anti-Pros (DSHB~ 1:10). Secondary antibodies were from Jackson Laboratories. After staining, discs were mounted in Vectastain and analyzed with a Zeiss confocal microscope. Adult eye sections were prepared as previously described (Yang et al., 1999). Wings were dehydrated in a 70% ethanol:30% glycerol solution and mounted in DPX (EMS sciences)

Biochemical analysis

For the GST pull-down assay the *ft* fragment was amplified by PCR and cloned in-frame with the N-terminal FLAG tag provided in the vector pFTX9. FLAG-Fat was then synthesized by in vitro translation using the TNT system (Promega). GST-Atro was produced by PCR amplification of a fragment starting at tyrosine 1639 and ending at the stop codon using primers with *Xho*I sites. After digestion with *Xho*I this fragment was cloned into pGex 5x. GST and the GST-Atro fusion were produced in BL21-DE3 bacteria (Invitrogen), extracted in PBS with excess of bacterial-specific protease inhibitors cocktail (Sigma) and purified using glutathione-coupled beads (Pharmacia).

For binding assays, equal amounts of FLAG-Fat were added to pre-equilibrated beads containing 5 μg of GST fusions in HMK buffer (Zhang et al., 2002) in 400 μl and were rotated at 4°C overnight. Beads were recovered, washed in HMK and analyzed by SDS-PAGE gels followed by western blotting with ECL chemoluminescence (Amersham). The following primary antibodies were used: mouse anti-FLAG (Sigma 1:2000), rabbit anti-Atro (1:500) and rabbit anti-GST (a gift from F. Miralles, 1:10000). HRP-conjugated secondary antibodies were from Amersham.

RESULTS

We conducted a genetic screen for genes involved in cell adhesion and planar polarity, based on the observation that alterations in cell adhesions within a clone of cells cause them to mix inefficiently with surrounding cells, resulting in a smooth-edged clone (Dahmann and Basler, 2000; Lawrence et al., 1999; Yang et al., 1999). We mutagenized flies and screened for mutations that, when homozygous, produce smooth edged clones (Fig. 1B) and, when sectioned, revealed planar polarity defects. Out of this screen we obtained two new alleles of *ft*, one new allele of *ds*, and mutations in two other genes (as yet unidentified). *ft* encodes a transmembrane protein that is a putative cell adhesion molecule, with multiple cadherin repeats, EGF repeats and laminin G repeats, as well as large cytoplasmic domain with no informative homologies (Fig. 2A) (Mahoney et al., 1991). Fat is an enormous molecule, with a predicted molecular weight of 560 kDa. Loss of *ft* leads to excessive growth of imaginal tissues, and has thus been long considered a tumor suppressor gene in *Drosophila* (Bryant et al., 1988). *ds* encodes an adhesion molecule with 27 cadherin repeats and an unrelated cytoplasmic domain (Clark et al., 1995).

ft and *ds* control ommatidial polarity

Fat and Ds have been shown to have roles in PP in the eye, wing and abdomen (Casal et al., 2002), and it has been proposed that

Ds binding to Fat modulates Fat function. Consistent with this proposal, we see that homozygous loss of either *ft* or *ds* randomizes PP (Fig. 1D,E).

A striking feature of clones of homozygous *ft* cells is that disruptions in PP are restricted to polar regions of the clone. In addition, entirely wild-type ommatidia on the polar side of the clone frequently show PP inversions (white arrow, Fig. 1F). Loss of *ft* does not disrupt polarity of wild-type tissue on the equatorial side of the clone, and in fact *ft* mutant tissue can be phenotypically rescued by adjacent wild-type tissue on the equatorial side of the clone (Rawls et al., 2002; Yang et al., 2002) (Fig. 1F).

Although loss of *ds* and *ft* throughout the eye produces similar PP defects, they have distinct clonal phenotypes. In *ds* clones, ommatida with disrupted polarity are primarily located on the equatorial region of the clone, and genotypically wild-type ommatida at the equatorial border of *ds* clones are often inverted in the dorsoventral axis. Remarkably, ommatidia at the polar edge of *ds* clones always adopt the correct polarity (Fig. 1G), suggesting that *ds* mutants can phenotypically rescued by wild-type tissue on the polar side of the clone.

Mosaic analysis of *ft* mutant clones has demonstrated a strong bias for the cell that retains *ft* function to become the R3 cell, whereas there is a bias for retaining *ds* function in the R4 cell (Rawls et al., 2002; Yang et al., 2002).

The cytoplasmic domain of Fat binds the transcriptional repressor Atro

To gain insight into how Fat controls PP, we searched for proteins that bind the cytoplasmic domain of Fat. We performed a yeast two-hybrid screen, using two different fragments of the Fat intracellular domain as baits to screen a *Drosophila* embryonic cDNA library. The bait for the first screen was a 160 amino acid fragment, close to the C terminus, whereas a non-overlapping fragment close to the transmembrane domain (green and black arrows; Fig. 2A) was used for the second screen. Both of these fragments cover regions of high homology to a human homolog of Fat (data not shown). *Drosophila Atrophin* (*Atro*) was isolated in the first screen, and specifically interacted with the Fat bait 1 (green arrow) but not with bait 2. *Atro* encodes a large protein of >200 kDa, with nuclear localization signals, putative DNA-binding and chromatin remodeling domains located at its N-terminus, and a region of particularly high homology to human Atrophins at the C terminus (Fig. 2A) (Erkner et al., 2002; Zhang et al., 2002). *Atro* is also known as *Grunge*. Atrophins have been shown to act as transcriptional repressors in *Drosophila* and in tissue culture studies (Wood et al., 2000; Zhang et al., 2002).

As Atro has been shown to act as a transcriptional repressor in the nucleus, while Fat is located at the cell membrane, such an interaction was unexpected. We confirmed the interaction between Fat and Atro through pull-down experiments, using a GST-Atro fusion protein, and in vitro translated, Flag-tagged Fat protein. A fragment of Fat, corresponding to yeast bait 1, binds specifically to a GST-Atro fusion protein, but not to GST alone (Fig. 2B). These data confirm our yeast 2-hybrid interaction, and provides additional support for a biochemical interaction between Atro and Fat.

ft and *Atro* show strong genetic interactions

To determine if the biochemical interaction between Fat and Atro is important in vivo, we looked for genetic interactions between *ft* and *Atro*, and found strong dominant genetic interactions. Heteroallelic combinations of a number of *ft* alleles are viable. Removal of one copy of *Atro* in this background severely compromises viability (Table 1). By contrast, loss of one copy of *Atro* in a wild-type background has no obvious effect on morphology or viability. This dominant heteroallelic lethality provides strong evidence for the biological importance of the interaction between Fat and Atro. To investigate if *ft* and *Atro* also show genetic interactions in PP, we have sectioned eyes from the few escapers obtained from crosses maintained at 18°C, and see consistent but subtle PP defects in ft^{GRV}/ft^{1}; $Atro^{35}$/+ heteroallelic combinations. The eyes of ft^{GRV}/ft^{1} flies and $Atro^{35}$/+ flies raised at the same temperature are entirely wild type (data not shown).

Table 1. *ft* and *Atro* interact genetically

ft allele	GRV (25°C)	GRV (18°C)	fd (18°C)	chance (18°C)
CyO	337	427	n.d.	457
ft^{*}/ft^{1}	120	164	n.d.	196
CyO+SM6:TM6	179	783	784	826
ft^{*}/ft^{1}; $Atro^{35}$/+	0	26	0	22

Female flies of $w;ft^{GRV}/CyO$, $w;ft^{fd}/CyO$ and $w;ft^{chance}/CyO$ genotypes were crossed to males of $w;ft^{1}/CyO$ (control, first 2 rows) and $w;ft^{1};Atro^{35}/SM6:TM6$ genotypes at 25°C or 18°C. The results are sums of two to four independent crosses.

When using a different allele of Atro, $Atro^{11}$, flies emerge in normal mendelian ratios for all genotypes; however, we observed a dramatic shortening of the adult flies' lifespan when one copy of the $Atro^{11}$ allele is present; ft^{GRV}/ft^{1}; $Atro^{11}$/+ flies have severely decreased viability, with most flies dying between day 4 and 8. As a result of this, a dramatic drop in viability is observed (Fig. 2C). A similarly shaped curve is obtained for ft^{chance}/ft^{1}; $Atro^{11}$/+ flies. Interestingly ft^{GRV}/ft^{1}; $Atro^{11}$/+ flies appear to have motor deficits as their general motility and climbing behaviors are severely reduced.

Atro is expressed in the eye disc and is found both in the nucleus and the cytoplasm

Atro has been shown to act as a transcriptional co-repressor in vivo in *Drosophila* (Zhang et al., 2002) and has been reported as a ubiquitously expressed nuclear protein (Zhang et al., 2002; Erkner et al., 2002). To gain some insight into how Atro might interact with a transmembrane protein such as Fat, we investigated its distribution in the eye imaginal disc using an affinity-purified antibody raised against the last 14 amino acids of the protein. This antibody reveals distinct nuclear staining in all photoreceptors behind the morphogenetic furrow, as well as in cells in front of the furrow (Fig. 2D). This staining is lost in *Atro* mutant clones (white arrow; Fig. 2E), confirming the specificity of the antibody. Reconstructed orthogonal views of confocal sections through imaginal discs that contain $Atro^{-}$ clones confirms that both the nuclear and non-nuclear staining is lost in *Atro* clones, indicating that Atro protein is normally present both in the cytoplasm and inside the nucleus (Fig. 2F). Human Atrophins are also present in both the nucleus and in the cytoplasm (Schilling et al., 1999).

Atro clones, like *ft* clones, disrupt PP on the polar border of the clone

Atro has been reported to affect PP in the eye (Zhang et al., 2002),

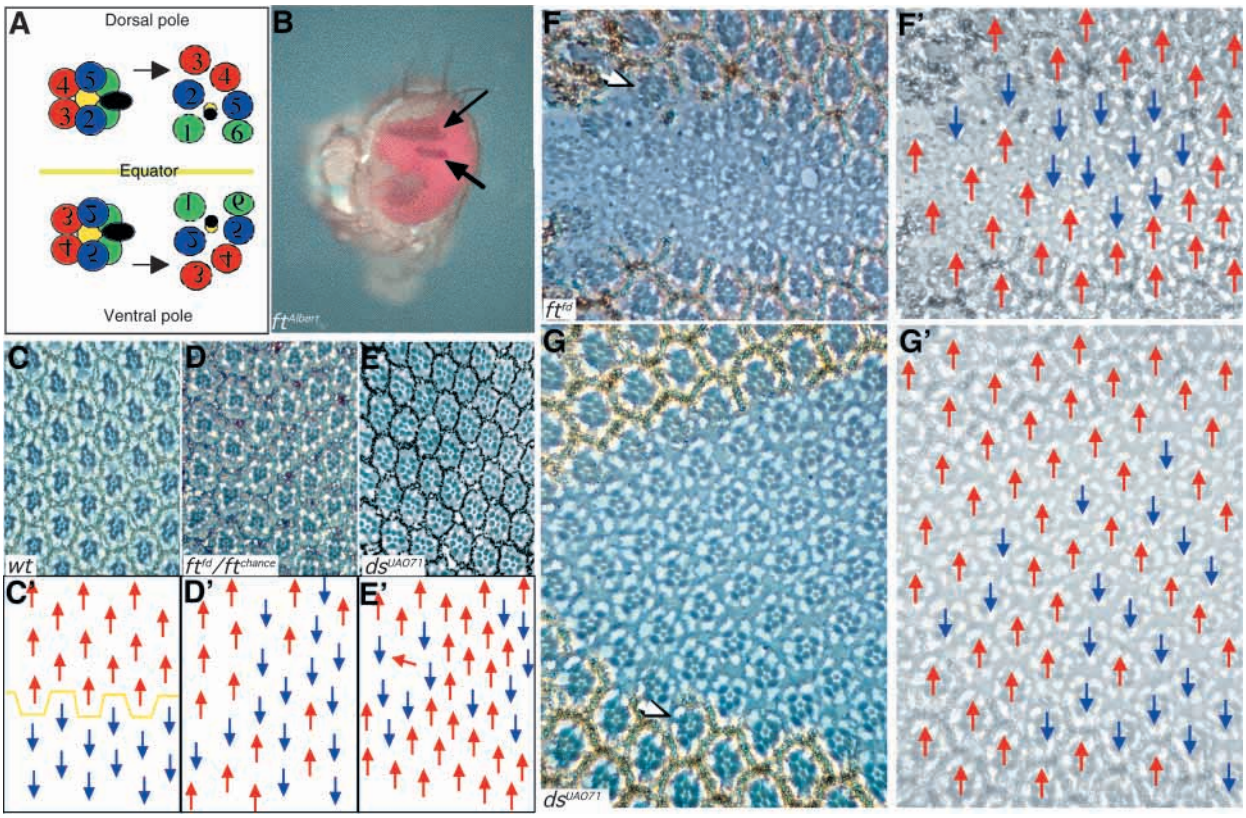

Fig. 1. *ft* and *ds* regulate planar polarity. (A) Wild-type dorsal (D) and ventral (V) ommatidia. At the five-cell stage, preclusters rotate in opposite directions to assume D and V polarity. Outer photoreceptors are recruited into the clusters as pairs and share similar characteristics, indicated by similar colors in the R1/6, R2/5 and R3/4 cells. Dorsal is upwards and anterior is leftwards. (B) Smooth edges of mitotic clones of ft^{Albert} (arrows). All *ft* alleles examined had smooth edges, planar polarity defects and enhanced growth in clones. (C-E′) Sections (C-E) and schematic diagrams (C′-E′) of wild-type, and *ft* and *ds* mutant fly eyes. In the wild-type eye (C,C′) the trapezoid shapes formed by the photoreceptor rhabdomeres of the D ommatidia point upwards (red arrows), the V ommatidia (blue arrows) point in the opposite direction; D and V fields are separated by a division known as the equator (yellow line). In ft^{fd}/ft^{chance} transheterozygous (D,D′) and ds^{UAO71} homozygous mutants (E,E′), D and V ommatidia are intermixed and no obvious equatorial line can be drawn. (F,G) Sections of ft^{fd} and ds^{UAO71} mutant clones and (F′,G′) diagrams of PP. ft^{-} and ds^{-} tissue are marked by the absence of pigment. White arrows indicates wild-type ommatidia on the polar (F) or equatorial (G) sides of the clones, non-autonomously affected by the clones. Red and blue arrows (F′,G′) indicate ommatidia with D and V polarity, respectively, in these and in all remaining panels.

but the nature of these defects have not been investigated in depth. To understand how Fat and Atro function in PP, we analyzed the planar polarity defects in *Atro* mutant clones in greater detail.

In $Atro^{-}$ clones, as in ft^{-} clones, we find non-autonomous alterations in polarity only on the polar border of the clone. Wild-type ommatidia at the polar border of dorsal *Atro* clones adopt a ventral appearance (Fig. 3A, white arrow), while wild-type and mosaic ommatidia at the equatorial border of the clone have normal polarity. Inside the clone there are significant defects in photoreceptor differentiation, suggesting that *Atro* has other roles in the eye in addition to the control of planar polarity. Analysis of homozygous clones of weaker *Atro* alleles, induced by insertion of a P element, shows very similar phenotypes (not shown).

Atro, like *ft*, is specifically required in the R3 photoreceptor

ft has been reported to be specifically required in the R3 photoreceptor (Yang et al., 2002). We assayed the requirements for *Atro* in different photoreceptors using clones of homozygous *Atro* cells generated in a heterozygous background. Because there are no strict lineage relationships among ommatidial cells, the ommatidia along the clonal border are composed of random combinations of $Atro^{+}$ and $Atro^{-}$ cells. Among these combinations were mosaic ommatidia in which only one member of the R3/R4 precursor pair possesses functional *Atro*. $Atro^{+}$ ommatidia can be identified by the presence of black pigment granules in the photoreceptor rhabdomeres (Fig. 3B,C). In virtually all cases in which an ommatidium that was located on the polar border of the clone and had incorrect polarity was mosaic for *Atro* in the R3/ R4 cell pair, the R3 photoreceptor retained Atro (black arrows Fig. 3B). This mosaic bias suggests that Atro is preferentially required in the R3 cell.

A careful quantitative analysis of these mosaic ommatidia (Table 2) shows a general bias for retaining the Atro function in all the anterior photoreceptors as previously reported for *ft* by Rawls et al. (Rawls et al., 2002). However, both in ommatidia that retained the correct polarity and inverted ommatidia, the bias for R3 is very strong and is significantly higher than that observed for the other anterior photoreceptors, R1 and R2.

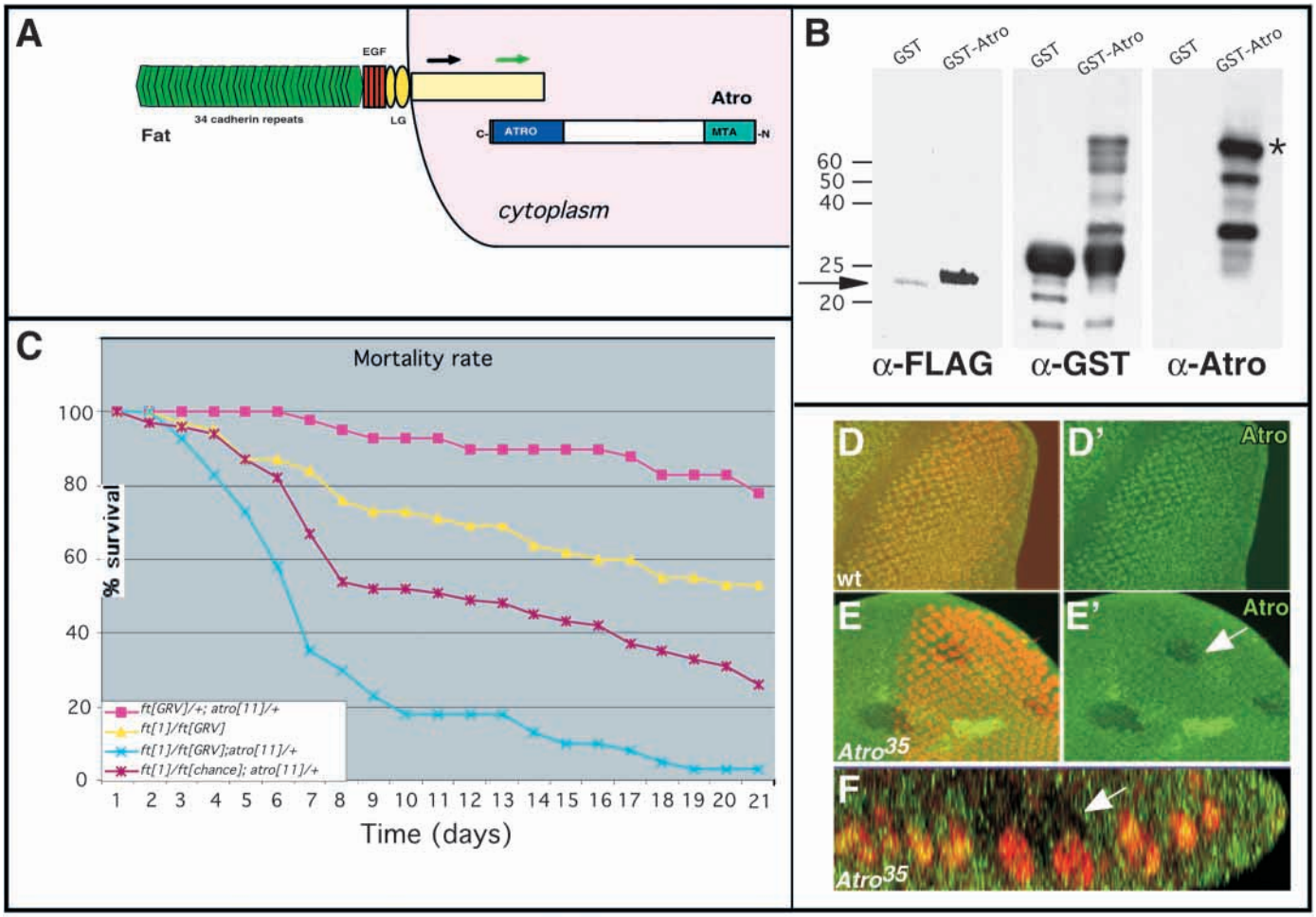

Fig. 2. Physical and genetic interaction between *Atro* and *ft*. (A) Diagram of Ft and Atro structures. Ft is a 560 kDa transmembrane protein with cadherin (green), EGF (red) and Laminin G (yellow) repeats and a novel cytoplasmic domain. Black and green arrows indicate fragments of Ft used in our Y2H. Atro interacts with the fragment indicated by the green arrow. Atro has strong homologies to human atrophins. This homology is especially high in the Atro domain (blue). Atro also contains regions found in transcriptional regulators known as MTA and SANT domain (cyan). (B) FLAG-Ft binds GST-Atro. Western blotting with anti-FLAG antibody reveals the amount of Ft pulled down by GST alone (left, in all panels) and GST-Atro (right, in all panels), respectively. Blotting with α-GST indicates the amounts of GST fusion proteins present. GST-Atro is degraded so that most of the protein produced is GST and very little protein is full-length Atro. Probing with α-Atro reveals which fragments of the degraded GST-Atro still contain Atro protein. Arrow indicates FLAG-Fat and asterisk marks full-length GST-Atro. (C) *Atro* dominantly enhances *ft* mortality rate. *w;ft^{GRV}/CyO* (control) and *w;ft^{1}/CyO* females were crossed to *w;Atro^{11}/TM6*, *w;ft^{1}/CyO*, *w;ft^{GRV};Atro^{11}/SM6:TM6* and *w;ft^{chance};Atro^{11}/SM6:TM6* males at 29°C. Flies of the correct genotypes were collected every day, kept at 22°C and put in new vials every 48 hours. The results are average of two independent crosses and based on a total number of 50 to 150 flies for each genotype. (D-F) Atro protein expression (green) in the eye imaginal disc. An antibody raised against the last 14 amino acids of the Atro protein reveals ubiquitous staining in all cells of a wild-type eye disc (D,D′), including the neuronal photoreceptors, marked by the Elav protein (red). The staining is partially lost within *Atro^{35}* clones (E,E′,arrow), both ahead and behind the morphogenetic furrow. (F) Orthogonal reconstruction of a series of confocal sections through the *Atro^{35}* clone shown in E′ (white arrow). Staining is visible in the cytoplasm and in the nuclei, and both are decreased in the clone.

Table 2. Quantification of *Atro* bias in photoreceptors of mosaic ommatidia

Clone border	Ommatidial polarity	$3^{+}4^{-}$	$3^{-}4^{+}$	$1^{+}/6^{-}\ 2^{+}/5^{-}$	$1^{-}/6^{+}\ 2^{-}/5^{+}$	$A^{+}P^{-}$	$A^{-}P^{+}$
Eq	Wild type (total)	63 (26)	37 (17)	53 (38)	47 (33)	61 (74)	39 (50)
Pol	Wild type	71 (10)	29 (4)	48 (14)	52 (15)	56 (24)	44 (19)
	Inverted	96 (27)	4 (1)	77 (20)	33 (6)	87 (47)	13 (7)
	Total	88 (37)	12 (5)	62 (34)	38 (21)	73 (71)	27 (26)
Eq+Pol	Total	74 (63)	26 (22)	57 (72)	43 (54)	64 (145)	36 (76)

Results expressed in percentage and total numbers (in parentheses) from 144 ommatidia mosaic for at least one PR pair. Columns 5 and 6 are a sum of mosaics for R1/6 and R2/5 pairs. Columns 7 and 8 are the sum of mosaics of all outer PR (R1/6, R2/5 and R3/4).

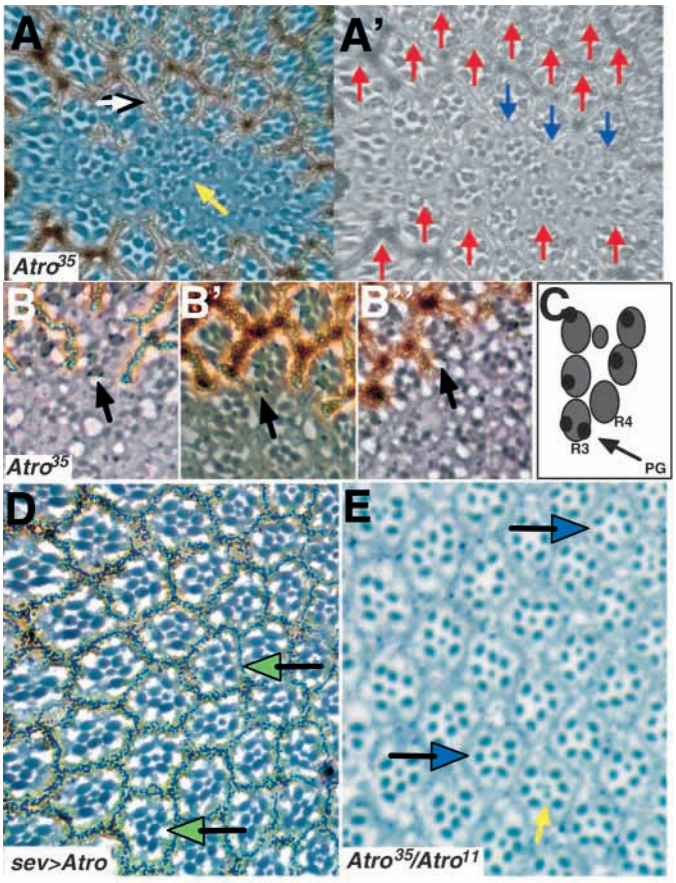

Fig. 3. *Atro*, like *ft*, is required for PP and in the R3 cell. (A) Section of a $Atro^{35}$ mutant clone and (A′) diagram of PP. The clone is marked by the absence of pigment. White arrow indicates a wild-type ommatidium, non-autonomously affected by the clone. The strong photoreceptor specification defects make it impossible to assess the polarity of most ommatidia inside the clone (yellow arrow). (B-B″) Close-ups of three ommatidia from $Atro^{35}$ clones with mosaic R3/R4 pair and schematic representation of such mosaics (C). The pigment granules (PG; marking the wild type) are always present on the R3 rhabdomere (black arrows) and never on the R4 cell in mosaic ommatidia. (D) Section through the eye of fly expressing *Atro* under *sev* control. Several ommatidia appear to have lost their chirality and have adopted a symmetric form of the R3/R3 type (green arrows). (E) Section through the eye of a viable combination of two different *Atro* mutations ($Atro^{35}/Atro^{11}$). Several ommatidia appear to have lost their chirality and have adopted a symmetric form of the R4/R4 type (blue arrows). Some ommatidia have extra inner photoreceptors (yellow arrow).

In addition, in viable heteroallelic combinations of *Atro* (Fig. 3E, black arrows) we frequently see symmetric ommatidia, mostly of the R4/R4 achiral subtype. Conversely, when a wild-type form of Atrophin is transiently overexpressed in the eye imaginal disc under the control of the *sevenless* enhancer – alongside alteration in the degree of rotation and the polarity of several ommatidia – many elongated symmetric ommatidia of the R3/R3 achiral subtype are observed (Fig. 3D). These phenotypes have been described for mutants in *fz* and *Notch* and strongly support the notion that Atro biases the R3/R4 cell fate choice towards R3.

Despite the similarity of the PP deficits, *Atro* clones do display some differences when compared with *ft* clones. As mentioned above, *Atro* is required for the survival or correct specification of photoreceptors. Ommatidia within the clones often appear to have lost one or more outer photoreceptors, and in many cases they have more than one inner photoreceptor with smaller rhabdomeres (Fig. 3A,E, yellow arrows).

Loss of either *Atro* or *ft* disrupts planar polarity in the eye disc

The autonomous and non-autonomous defects in *ft* clones are first detectable in the eye imaginal disc, using antibodies against Bar, a marker for R1 and R6 (Higashijima et al., 1992) (Fig. 4A). Ommatidia with a dorsal orientation are indicated with red arrows; ventral orientation is indicated with blue arrows. Although PP is disrupted throughout much of the *ft* clones, there is often a striking rescue of ommatidial orientation on the equatorial border of the *ft* clone. This has led to the proposal that a *ft*-dependant signal is carried for one or two ommatidial rows from the Ft^{+} cells outside the clone (Rawls et al., 2002). This phenotype is reversed in *ds* clones, where there is a clear rescue of the mutant ommatidia at the polar border, whereas the polarity defects spread into the wild-type tissue for up to two rows at the equatorial border of the clone (Fig. 4B)

We investigated Atro function in the eye imaginal disc, using the polarity marker, *E(spl)mδ0.5* (Cooper and Bray, 1999). In wild-type ommatidia *E(spl)mδ0.5* is expressed in the polar cell, which becomes specified as R4. *Atro* mutant clones (marked by loss of GFP) show disruptions of the regular pattern of planar polarity, as revealed by the position of the R4 marker within an ommatidium. Within $Atro^{-}$ ommatidial clusters the cell expressing the R4 marker frequently occupied the position normally taken by the equatorial cell (black arrows), indicating that these ommatidia had switched their dorsoventral PP (Fig. 4C). Strikingly, there are non-autonomous disruptions in PP in the wild-type tissue on the polar border of the clone. The alteration of ommatidial polarity in $Atro^{-}$ ommatidia and in surrounding tissue is diagramed in the adjacent panel (Fig. 4C′). It is clear that *Atro* clones (like *ft* clones) show an equatorial rescue of normal PP within the clone, and non-autonomous disruptions of planar polarity at the polar border of the clone.

We also saw, at lower penetrance, alterations in the ability of Atro photoreceptors to commit to the R3 cell versus R4 cell fate in the imaginal disc. Fifteen percent of ommatidia in $Atro^{35}$ clones show additional photoreceptors with an R4 cell marker, suggesting that these ommatidia have adopted an R4/R4 fate. Only 2% of *Atro* ommatidia have lost the R4 cell marker, which may suggest they have adopted an R3/R3 fate. In flies with the weaker, viable combination of Atro alleles ($Atro^{35}/Atro^{11}$), the same tendency is seen, though less strongly: Out of 610 ommatidia analyzed for expression of the R4 marker, 49 were of the R4/R4 class and five were of the R3/R3 type (data not shown). This tendency of *Atro* ommatidia to adopt an R4/R4 configuration is seen throughout clones, without any evidence for equatorial rescue. Together, these data support a cell-autonomous function for Atro in R3 fate determination.

Atro and *ft* are required to repress four-jointed in the eye

ft has been shown to repress expression of *fj*, which encodes a

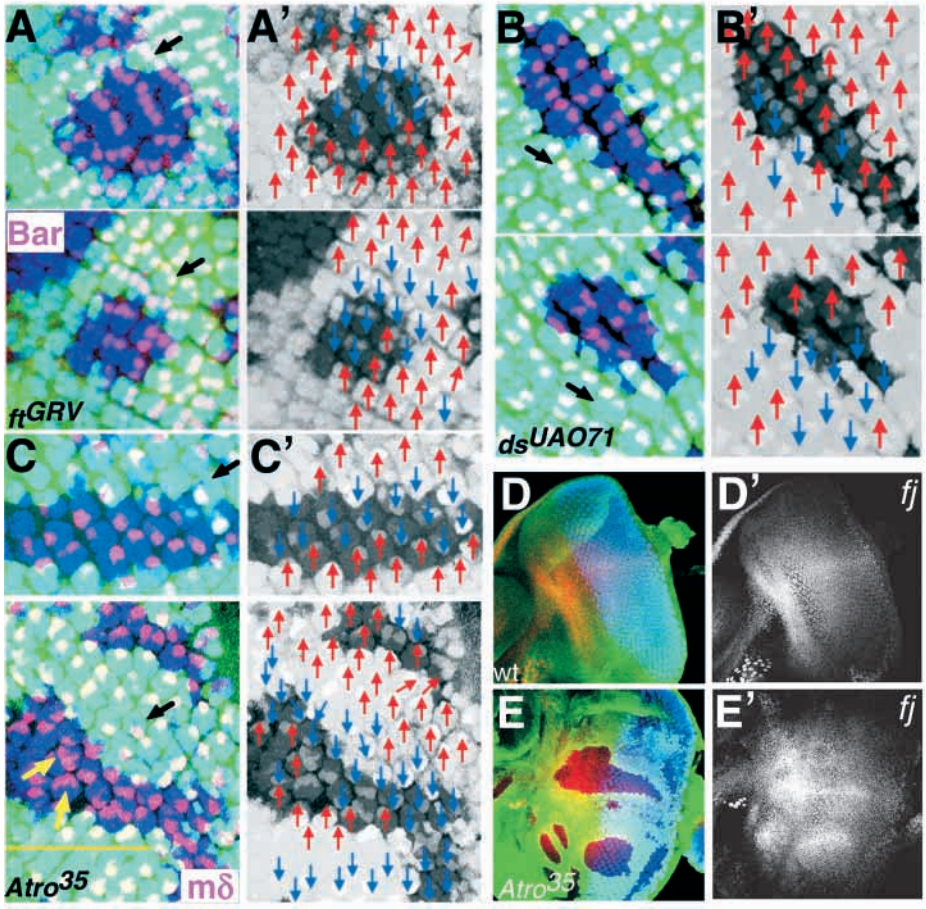

Fig. 4. Ft, Ds and Atro control planar polarity in the eye imaginal disc. In all panels, clones are marked by the absence of GFP (green). Elav (blue) is a marker for all neuronal photoreceptor nuclei. All pictures are vertical projections of several confocal sections. (A,A′) Loss of *ft* alters PP within and outside the clone. Bar (red) highlights the R1/R6 pair of photoreceptors. Black arrows indicates wild-type ommatidia, non-autonomously affected by the clone. (A′) Arrows indicate ommatidia with D (blue) and V (red) PP. (B,B′) Loss of *ds* alters PP within and outside the clone. ds^{UAO71} mutant clones and diagram of ommatidial polarity. Bar (red). Black arrows indicate wild-type ommatidia non-autonomously affected by the clone. (C,C′) Loss of *Atro* alters PP within and outside the clone $Atro^{35}$ mutant clones and diagram of PP. The β-Gal from *mδ-lacZ*, a marker for the R4 cell (red). The endogenous equator is indicated by a yellow line. Black arrows point to wild-type ommatidia, non-autonomously affected by the clone. In several clusters more than one cell expresses β-Gal (yellow arrows). (D,E′) *fj* transcription is controlled by Atro. Expression of *fj-lacZ* (red in D and E, white in D′ and E′) in wild-type (D,D′) and in a $Atro^{35}$ mutant clones (E,E′). β-Gal is strongly upregulated in *Atro* mutant tissue. Note that inside *Atro* clones *fj-lacZ* maintains its gradient-shape expression, with higher levels on the part of the clone closer to the midline.

type II transmembrane/secreted protein, expressed in a graded fashion from the equator towards the pole of the eye imaginal disc (Fig. 4D) (Brodsky and Steller, 1996; Buckles et al., 2001; Villano and Katz, 1995; Yang et al., 2002; Zeidler et al., 1999; Zeidler et al., 2000). *fj* has been implicated in the regulation of ommatidial polarity, based on the observation that reversals of ommatidial polarity occur along the polar border of *fj* mutant clones. In addition ectopic expression of Fj in clones can also produce reversals of ommatidial polarity. Together these data suggest that ommatidia can recognize and polarize to a gradient of Fj protein.

Atro has been shown to act as a transcriptional repressor (Zhang et al., 2002). To see if the ability of *ft* to repress *fj* could be mediated by *Atro*, we examined *Atro*⁻ clones using *fj-lacZ* to monitor changes in *fj* transcription. We found that loss of *Atro* (Fig. 4E), like loss of *ft* (Yang et al., 2002) results in an increase in *fj* transcription, demonstrating that Atro is needed for the proper regulation of the *ft* target *fj*.

Atro has additional roles in PR specification not seen in *ft* clones

Atro adult clones have clear disruptions in photoreceptor specification and/or survival (Fig. 3A). These defects include loss of outer photoreceptors and extra inner photoreceptors. To determine if *Atro* is functioning in cell fate decisions important for photoreceptor specification, we stained *Atro* mutant clones with antibodies that recognized specific subsets of photoreceptors. Loss of outer photoreceptors is a common feature of *Atro* mutant clones in the adult, therefore we examined expression of Bar, a marker for the R1 and R6 outer photoreceptors. In *Atro*⁻ clones Bar staining is variable, and at times only one cell expresses Bar (Fig. 5A, yellow arrowheads). Ommatidia in adult *Atro* clones often also have extra inner photoreceptors. To investigate if these extra inner photoreceptors represented extra R7-like cells, we examined *Atro* clones for Prospero, which is expressed in the R7 cell and in cone cells (Kauffmann et al., 1996). In *Atro* clones, additional photoreceptor cells express Prospero (Fig. 5B, white arrows), compared with surrounding heterozygous tissue, suggesting that in the absence of *Atro*, outer photoreceptors were transformed into R7-like photoreceptors [defects that we never find in *ft* clones (data not shown)]. Therefore *Atro* is needed for fate specification for both inner and outer photoreceptor classes.

Another difference between *ft* and *Atro* function lies in the control of growth. Loss of *ft* leads to a loss of growth control, which is reflected in the greater size of mutant tissue (marked by the loss of GFP) compared with the twin spot, which has two copies of the GFP marker (yellow arrows; Fig. 5D) and is brighter than the surrounding heterozygous tissue. By contrast, *Atro*⁻ clones (Fig. 5C) are similar in size to their twin spot, suggesting that they lack the tumor suppressor phenotype of *ft* clones.

Finally, one striking feature of *ft* clones is their round and smooth appearance, which is visible in clones in the adult, and in the eye imaginal disc (Fig. 1B, Fig. 5D). Although *Atro*

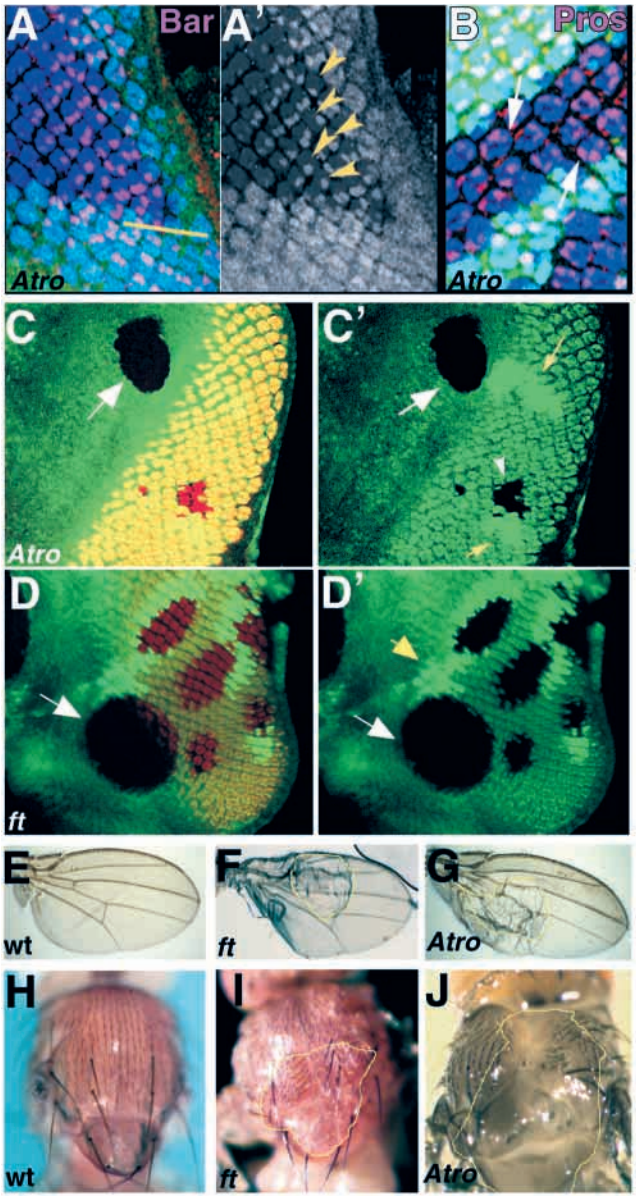

Fig. 5. Atro and Ft act separately in some developmental processes and together in others. (A,A′,B) Photoreceptor specification defects in *Atro*^{35} mutant clones in the eye imaginal disc. The endogenous equator is marked by the yellow line. Bar staining (A) in red. Yellow arrows (A′) designate clusters in which only one cells stains for Bar, indicating loss of R1 or R6 cell fate. Staining for the Prospero (Pros; red in B) a nuclear protein (a marker for R7 and the cone cells) reveals that in several clusters more than one cell has adopted the R7 fate (white arrows). Although the cone cells are mostly located above the plane of this section some of their nuclei (identified by their elongated shape) are present in this picture. (C,C′) *Atro*^{35} mutant clone marked by the absence of GFP (green). Note the round shape of the clone in front of the morphogenetic furrow (white arrows in C and C′) compared with the irregular shape of a clone behind the furrow (small arrowhead in C′) and of the twinspots, recognizable because of the brighter green staining due to the double amount of GFP (yellow arrows in C′) Elav(red). (D,D′) *ft*^{GRV} mutant clone marked by the absence of GFP (green), Elav (red). Note the round shape of all the clones both in front of and behind the morphogenetic furrow (white arrows) compared to the irregular shape of the twinspots (yellow arrow). (E-G) Pictures of *wt* wings (E) or wings carrying *ft*^{GRV} (F) or *Atro*^{35} (G) mitotic clones. *ft* and *Atro* clones (broken yellow lines) generate blisters in which the dorsal and ventral sheet of the wing are separated. (H-J). Dorsal thoraces of a wild-type fly (H) or flies with *ft*^{GRV} (I) or *Atro*^{35} (J) clones (broken yellow lines). Note the cleft in the thorax, indicating incomplete fusion of the left and right imaginal discs.

clones do not appear smooth in the adult, *Atro* clones in the eye disc appear strikingly smooth when they are located anterior to the morphogenetic furrow (Fig. 5C, white arrow). Comparison with the twin spot (yellow arrow), confirms that this effect is specific to loss of *Atro*. This smoothness is lost after progression of the furrow, when ommatidial differentiation commences (marked by Elav staining in red), suggesting that *Atro* acts specifically in a pre-furrow adhesion process that is lost upon neuronal differentiation.

ft and *Atro* act together in other tissues

There are a number of similarities in mutant phenotypes that suggest that *Atro* and *ft* function together at several stages in development. Atro is expressed ubiquitously throughout embryonic and larval development, and is also maternally contributed (Erkner et al., 2002; Zhang et al., 2002). *ft* is also maternally contributed, and is expressed in most cells in the embryo and the larva. Clones of *ft*^{GRV} in the wing produce blisters where the dorsal and ventral surfaces of the wing fail to fuse (Fig. 5F) (Garoia et al., 2000). Small clones of *Atro* have been reported to result in swirls of wing hairs and in notching when they touch the dorsoventral border (Zhang et al., 2002). We observed these defects, and in addition we noted that when we induced *Atro*^{35} clones earlier in development, these clones also formed blisters that are similar to those found in *ft* clones (Fig. 5G). Thoracic clones of *Atro* disrupt thorax closure (Zhang et al., 2002) (Fig. 5J). Loss of *ft* in clones also disrupts thorax closure (Fig. 5I). Taken together, these data suggest that Fat and Atro may function together many times during development.

DISCUSSION

We describe a novel interaction between a cell adhesion molecule, Fat and a nuclear transcriptional co-repressor, Atro. We demonstrate that Fat and Atro act together in a variety of tissues, display strong genetic interactions, and are essential for cell adhesion, and cell fate choices during the development of planar polarity in the fly eye. We show that *ft* and *Atro* function in control of a planar polarity signal, and in the R3 fate determination. There is precedence in the eye for the reiterative role of genes acting at different stages in the development of planar polarity. Like Atro, Notch acts early at the midline to upregulate the expression of *fj*. Later, in a separate mechanism that is coincident with ommatidial rotation, Notch defines the R4 cell fate and promotes correct rotation of the precluster.

ft and *Atro* bias towards an R3 fate

Mosaic analysis of *ft* mutant clones demonstrated a strong bias for the cell that retains *ft* function to become the R3 cell (Rawls et al., 2002; Yang et al., 2002). This has been interpreted to indicate that Fat directly biases the cell to become an R3 cell

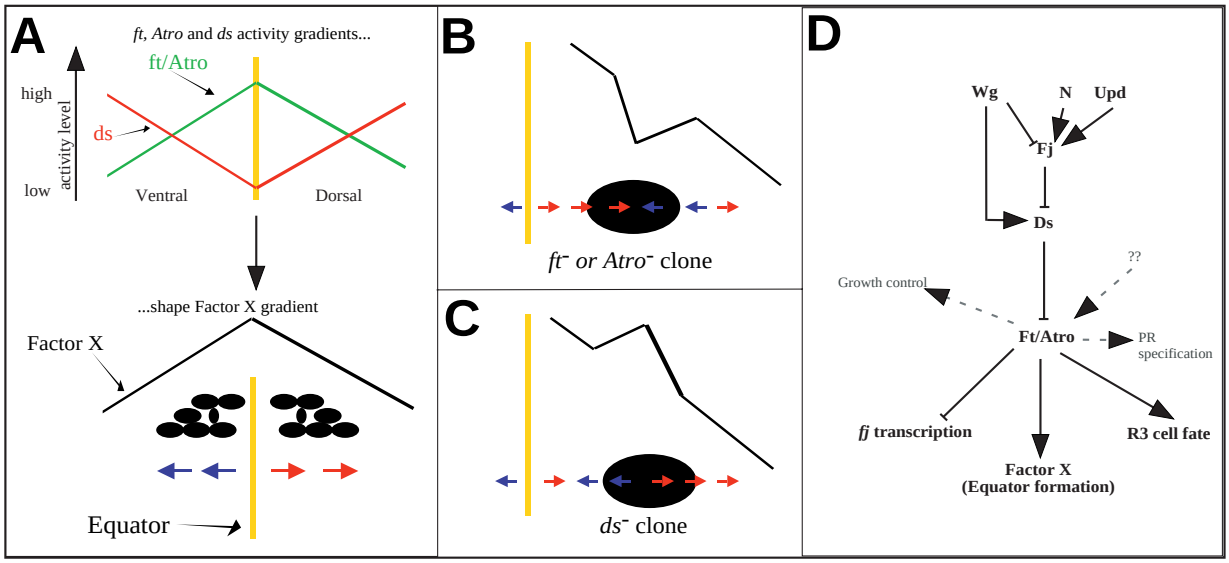

Fig. 6. Model for *ds*, *ft* and *Atro* in PP establishment. (A) Model for how *ft/Atro* (green) and *ds* (red) activity gradients relate to Factor X gradient (black), which is instructive for PP. *ds* activity is high at the D and V regions of the disc and reaches its minimum at the DV midline. Ft/Atro promote production of Factor X, and Ds inhibits it, probably by inhibiting Ft. As a result, Factor X production will be highest at the midline and lowest at the edges. (B) Effects on Factor X gradient and ommatidial polarity of a *ft* or *Atro* clone. The clone (black ellipse) generates a sink in the Factor X gradient. Outside the clone, on the polar side a new maximum of Factor X is created. (C) Effects on Factor X gradient and ommatidial polarity of a *ds* clone. *ds* clone is predicted to produce excess Factor X, altering the slope of the gradient, and reorganizing the ommatidia accordingly. (D) Model for Atro function in PP. Initially, Wg (expressed at the D and V poles), N (active at the D/V midline) and Unpaired (Upd) (secreted centrally) set up Fj expression gradient with its peak at the midline. Wg also promotes *ds* expression. Ft and Atro are responsible for the production of Factor X, the promotion of the R3 versus the R4 cell fate and the repression of *fj* transcription. In addition to their requirement in PP, Ft and Atro control separate activities (broken gray arrows).

(Yang et al., 2002). We find that *Atro* clones also show a bias for the R3 cell to retain Atro function, supporting the model that Atro, like Fat, works in R3 fate determination.

However, an extensive mosaic analysis found that all anterior cells (R1, R2 and R3) tend to be ft^{+}, and all posterior cells (R4, R5 and R6) tend to be ft^{-} (Rawls et al., 2002). Rawls et al. suggested that this bias is due to spatial considerations, cells that are polar in the precluster, undergo a 90° rotation, leaving them in a posterior position in the adult. At the polar border of *ft* clones, ommatidia rotate in the opposite direction to wild type, therefore the bias is reversed, leading to an increase in ft^{-} anterior cells. Therefore, they concluded that additional data was required to show that *ft* function is specifically needed in R3. To determine if *ft* and *Atro* are specifically required in the R3 photoreceptor, we have undertaken mosaic analysis of *Atro*, *ft* and wild-type clones. We find that in wild-type clones, marked only by *white*, ommatidia at the polar border of the clone show a weak preference for posterior photoreceptors to be wild-type (60.75±4.7%; P over A). This bias is strictly due to the spatial constraints of recruitment in clones. In *ft* clones, we find that at the equatorial border (where polarity is unaltered) there is no discernable difference between anterior photoreceptors subclass types; 85% of all photoreceptors that retain *ft* are anterior class. The increase from ~61% to 85% is probably due to the adhesive properties of *ft*, which result in smooth edged clones.

By contrast, at the polar border, which is where planar polarity is altered, there is a marked tendency for *ft* function to be retained specifically in the R3 photoreceptor; 100% of R3 cells retained *ft*, whereas only 83% of all anterior photoreceptors retained *ft*. Our mosaic analysis of *Atro* clones showed that the bias introduced by PP alterations at the polar border of clones (similar to *ft*) introduces a general bias for anterior photoreceptors. However, again, the bias is stronger in the R3 cell than for other anterior photoreceptors. This increased bias in the R3 photoreceptor over the other anterior class member suggests that *ft* and *Atro* are important in R3 fate.

The conclusion that Atro function is important for the R3 cell fate is also strongly supported by our observation that loss of *Atro* often results in symmetric ommatidia with two R4 cells. This is reflected by the increase in R4/R4 ommatidia seen in *Atro* clones in the eye disc marked by expression of the R4 marker, *md-lacZ*. In addition the overexpression of Atro in R3 and R4 generates symmetric ommatidia with two R3 cells. Together, these data support the proposal that Atro is needed for the R3 fate.

The non-autonomous nature of the PP defects associated with *ft* and *Atro* mutant clones could have presented some problems to mosaic analysis. We might have expected that non-autonomous alterations in polarity would equally affect all photoreceptors, yet our data clearly show enhanced requirements for *ft* and *Atro* function in the R3 photoreceptor over other photoreceptors. In addition, the proposal that Atro is needed for the R3 cell fate is supported by our analysis of the R4 marker in eye discs. Interestingly, the tendency to lose the R3 cell fate in *Atro* clones is seen throughout the clone, and does not appear to participate in the phenomena of equatorial rescue or polar nonautonomy.

Because Fz is also needed for R3 fate decisions, it has been

suggested that Fat positively affects Fz signaling (Yang et al., 2002). Our observation that Atro acts with Fat and also biases towards the R3 fate suggests that the regulation of Fz by Fat may not be direct. We propose instead that Atro is necessary for the *ft*-dependent bias to an R3 cell fate and for the production of a diffusible PP molecule that controls Fz activity.

The proposal that Fat increases Fz activity, and thereby biases a cell towards the R3 fate (Yang et al., 2002), does not explain the non-autonomous disruptions of wild-type tissue on the polar side of *ft* and *Atro* clones, or the rescue of *ft* and *Atro* mutant tissue from wild-type tissue on the equatorial side of the clone. There are several models that could explain the non-autonomous disruptions of planar polarity. One model suggests that planar polarity is established through a 'domino effect'. This model is suggested by the striking accumulation of planar polarity components, such as Fz and Dsh on the distal edge of every cell in the wing (reviewed by McNeill, 2002). This observation, coupled with genetic data that suggests that high Fz activity on one side of the cell forces low Fz activity on the other side, leads to a model in which accumulation or loss of polarity in a cell leads to templating of that state onto the next cell, non-autonomously propogating PP defects. However in the eye, Fz and Dsh only show differential distribution on a subset of ommatidial precursor cells, and, importantly, intervening cells show no altered accumulation. These data argue against a simple templating model for PP in the eye.

An alternative model proposed by Rawls et al. (Rawls et al., 2002) suggests that the juxtapositioning of ft^+ and ft^- tissue contributes to midline determination and emphasizes the role of Fat in inhibiting DV signaling away from the equator. This inhibition would be relieved at the equator by an unidentified molecule that would inhibit Fat function. If this model was correct, a small *ft* clone should mimic the situation at the equator, where Fat function is predicted to be locally inhibited. We would therefore expect to find an ectopic equator in the middle of the clone. Instead, however, we observe the opposite phenotype, as the ommatidia on the two sides of the clone point towards the middle of the clone, rather than away from it.

A model for the function of *ft*, *ds* and *Atro* in establishing ommatidial polarity

We believe that the model that best explains both the equatorial rescue and polar nonautonomy of *ft* and *Atro* clones is that Fat and Atro together control expression of a planar polarity morphogen, here called 'factor X'. We imagine that factor X is in a gradient with high levels at the equator and low levels at the poles, thus all ommatidia will appear to 'point' down this gradient (see Fig. 6). If Fat and Atro are essential to the production of factor X, then the *ft/Atro* mutant tissue will be void of factor X, producing a sink in the gradient. The gradient will still be pointing in the same direction initially, thus the wild-type polarity of ommatidia at the equatorial side of the clone and 'equatorial rescue' seen in *ft* and *Atro* clones. For ommatidia at the polar edge of the clone, the gradient will be reversed, and ommatidia will point in the opposite direction. The gradient will also be disrupted outside of the clone, leading to inversions of the polarity of wild-type tissue on the polar side of the clone and 'polar nonautonomy' seen in these mutant clones. In large clones, there will be a region in the center of the clone where there is no detectable factor X, and as a result polarity will be randomized. All of these predictions are met in *ft* and *Atro* clones. Loss of Ds, which inhibits Fat function, should increase factor X. As predicted by this model, *ds* clones show disruptions in wild-type tissue on the equatorial side of the clone, and rescue of mutant tissue on the polar side of the clone. Without *ft* or *ds* function there would be no gradient and, consistent with this prediction, we see complete loss of planar polarity in eyes that are homozygous for strong alleles of *ft* or *ds*.

A gradient of Wg protein (which is high at the poles and low at the equator) initially establishes a gradient of Ds protein over the eye field (Yang et al., 2002). This gradient of Ds protein in turn produces a gradient of Fat activity, which, we believe, creates a gradient of Atro activity. We propose that each cell will produce factor X at a level that is proportionate to the level of Atro activity, which varies according to the position of that cell in the *ds* and *ft* activity gradients. Our model assumes that Factor X is a short-range diffusible molecule, which provides polarity information to ommatidial preclusters to direct their rotation. As Fat has been shown to be upstream of Fz, we speculate that the Atro-dependant Factor X is a ligand for Fz.

Atro and *ft* also act in different pathways

Both *ft* and *Atro* also act in other, apparently unrelated, pathways. One of the prominent features of *ft* mutant larvae is the loss of growth control, which leads to dramatically overgrown discs (Bryant et al., 1988) and mutant clones that are markedly larger than their sister twin spots (see Fig. 5D). However, $Atro^-$ clones do not display overgrowth in the eye, suggesting that *ft* restricts growth via an Atro-independent pathway. In addition, in the adult eye *Atro* clones (unlike *ft* clones) show severe defects in photoreceptor number and type, suggesting Atro has additional roles in photoreceptor specification and/or survival that are not shared by Fat. One particularly surprising result was our finding that $Atro^-$ clones are markedly smooth before the furrow, and that this smoothness is lost after the furrow passes. This suggests that Atro may function in a cell adhesion process that is lost upon cell differentiation.

Atro is a transcriptional repressor

Dentatorubral-pallidoluysian atrophy (DRPLA) is a dominantly inherited neuronal degenerative disease characterized by the variable combination of ataxia, choreoathetosis, myoclonus, epilepsy and dementia. This disease is caused by the expansion of a polyglutamine tract within the Atrophin 1 protein (Koide et al., 1994; Nagafuchi et al., 1994). Atro is the sole fly homolog of human atrophins. Atro has been shown to act as a transcriptional co-repressor in vivo in *Drosophila* (Zhang et al., 2002). Atro interacts genetically with *even skipped*, a transcriptional repressor, and is required for the in vivo repressive activity of *even skipped*. The transcriptional repressor activity of Atro has been localized to the highly conserved C-terminal region of Atro. This C-terminal region can bind to Evenskipped in vitro and interacts with the minimal repression domain of Evenskipped (Zhang et al., 2002).

We have shown here that the intracellular domain of Fat binds the C-terminal domain of Atro. The cytoplasmic expression of Atro and its interaction with Fat raises the possibility that instead of acting as a simple co-repressor, Atro functions in a more complex manner. Other transcriptional co-

repressors are known to be converted to transcriptional activators upon cell signaling, and future work will determine if the interaction of Fat with Ds alters the transcriptional activity of Atro.

Owing to the fact that Atro binds the cytoplasmic domain of Fat, we favor a model in which Atro acts downstream of Fat, possibly relaying a Fat-dependant signal to the nucleus. However, the similarity of the *ft* and *atro* loss-of-function phenotypes makes classical epistasis experiments difficult, therefore we cannot exclude a model in which *Atro* acts upstream of *ft*. Examination of the amount or subcellular distributions of Fat and Atro, suggest that *Atro* does not control Fat expression or localization, nor does *ft* control the levels or subcellular localization of Atro (data not shown).

In conclusion, we have demonstrated a novel interaction between a cell adhesion molecule, Fat, and a nuclear co-repressor, Atro, which work together in the control of planar polarity in the fly eye. We show that *Atro* is essential for the regulation of a previously identified *ft* target, *fj*, and acts in R3 cell fate determination. Based on these data, we propose that Fat and Atro act together to control the production of a diffusible planar polarity signal and to bias photoreceptors towards the R3 cell fate.

We dedicate this paper to the memory of Kirsten Hardiman, who died during the course of this work. We also thank Sarah Bray, Peter Bryant, Mike Simon and Tian Xu for fly stocks and antibodies. This manuscript was improved by comments from Jeff Axelrod, Julian Lewis, David Ish Horowicz, Sally Leevers, Caroline Hill and members of the McNeill laboratory. This work was supported by Cancer Research UK (Cancer Research UK was formed by a merger between the ICRF and the CRC in February 2002). M. F. was supported by a Marie Curie EU Fellowship.

REFERENCES

Aldler, P. N. and Lee, H. (2001). Frizzled signaling and cell-cell interactions in planar polarity. *Curr. Opin. Cell Biol.* **13**, 635-640.

Adler, P. N., Vinson, C., Park, W. J., Conover, S. and Klein, L. (1990). Molecular structure of frizzled, a Drosophila tissue polarity gene. *Genetics* **126**, 401-416.

Axelrod, J. and McNeill, H. (2002). Coupling planar cell polarity signaling to morphogenesis. *The Scientific World* **2**, 434-454.

Axelrod, J. D. (2001). Unipolar membrane association of Dishevelled mediates Frizzled planar cell polarity signaling. *Genes Dev.* **15**, 1182-1187.

Brodsky, M. H. and Steller, H. (1996). Positional information along the dorsal-ventral axis of the Drosophila eye: graded expression of the four-jointed gene. *Dev. Biol.* **173**, 428-446.

Bryant, P. J., Huettner, B., Held, L. I., Jr, Ryerse, J. and Szidonya, J. (1988). Mutations at the fat locus interfere with cell proliferation control and epithelial morphogenesis in Drosophila. *Dev. Biol.* **129**, 541-554.

Buckles, G. R., Rauskolb, C., Villano, J. L. and Katz, F. N. (2001). Four-jointed interacts with dachs, abelson and enabled and feeds back onto the Notch pathway to affect growth and segmentation in the Drosophila leg. *Development* **128**, 3533-3542.

Casal, J., Struhl, G. and Lawrence, P. (2002). Developmental compartments and planar polarity in Drosophila. *Curr. Biol.* **12**, 1189.

Clark, H. F., Brentrup, D., Schneitz, K., Bieber, A., Goodman, C. and Noll, M. (1995). Dachsous encodes a member of the cadherin superfamily that controls imaginal disc morphogenesis in Drosophila. *Genes Dev.* **9**, 1530-1542.

Cooper, M. T. and Bray, S. J. (1999). Frizzled regulation of Notch signalling polarizes cell fate in the Drosophila eye. *Nature* **397**, 526-530.

Dahmann, C. and Basler, K. (2000). Opposing transcriptional outputs of Hedgehog signaling and engrailed control compartmental cell sorting at the Drosophila A/P boundary. *Cell* **100**, 411-422.

Das, G., Reynolds-Kennedy, J. and Mlodzik, M. (2002). The atypical cadherin Flamingo links Frizzled and Notch signaling in Planar Polarity Establishment in the Drosophila eye. *Dev. Cell* **2**, 1-20.

Erkner, A., Roure, A., Charroux, B., Delaage, M., Holway, N., Core, N., Vola, C., Angelats, C., Pages, F., Fasano, L. and Kerridge, S. (2002). Grunge, related to human Atrophin-like proteins, has multiple functions in Drosophila development. *Development* **129**, 1119-1129.

Fanto, M. and Mlodzik, M. (1999). Asymmetric Notch activation specifies photoreceptors R3 and R4 and planar polarity in the Drosophila eye. *Nature* **397**, 523-526.

Garoia, F., Guerra, D., Pezzoli, M., Lopez-Varea, A., Cavicchi, S. and Garcia-Bellido, A. (2002). Cell behavior of Drosophila Fat cadherin mutations in wing development. *Mech. Dev.* **94**, 95-109.

Higashijima, S., Kojima, T., Michiue, T., Ishimaru, S., Emori, Y. and Saigo, K. (1992). Dual Bar homeo box genes of Drosophila required in two photoreceptor cells, R1 and R6, and primary pigment cells for normal eye development. *Genes Dev.* **6**, 50-60.

Kauffmann, R. C., Li, S., Gallagher, P. A., Zhang, J. and Carthew, R. W. (1996). Ras1 signaling and transcriptional competence in the R7 cell of Drosophila. *Genes Dev.* **10**, 2167-2178.

Koide, R., Ikeuchi, T., Onodera, O., Tanaka, H., Igarashi, S., Endo, K., Takahashi, H., Kondo, R., Ishikawa, A., Hayashi, T. et al. (1994). Unstable expansion of CAG repeat in hereditary dentatorubral-pallidoluysian atrophy (DRPLA). *Nat Genet.* **6**, 9-13.

Lawrence, P. A., Casal, J. and Struhl, G. (1999). The hedgehog morphogen and gradients of cell affinity in the abdomen of Drosophila. *Development* **126**, 2441-2449.

Mahoney, P. A., Weber, U., Onofrechuk, P., Biessmann, H., Bryant, P. J. and Goodman, C. S. (1991). The fat tumor suppressor gene in Drosophila encodes a novel member of the cadherin gene superfamily. *Cell* **67**, 853-868.

McNeill, H. (2002). Planar polarity: location, location, location. *Curr. Biol.* **12**, R449-R451.

Nagafuchi, S., Yanagisawa, H., Ohsaki, E., Shirayama, T., Tadokoro, K., Inoue, T. and Yamada, M. (1994). Structure and expression of the gene responsible for the triplet repeat disorder, dentatorubral and pallidoluysian atrophy (DRPLA). *Nat Genet.* **8**, 177-182.

Park, W. J., Liu, J. and Adler, P. N. (1994). The frizzled gene of Drosophila encodes a membrane protein with an odd number of transmembrane domains. *Mech Dev.* **45**, 127-137.

Rawls, A., Guinto, J. B. and Wolff, T. (2002). The cadherins, Fat and Dachsous, regulate dorsal/ventral signaling in the *Drosophila* eye. *Curr. Biol.* **12**, 1021-1026.

Schilling, G., Wood, J. D., Duan, K., Slunt, H. H., Gonzales, V., Yamada, M., Cooper, J. K., Margolis, R. L., Jenkins, N. A., Copeland, N. G. et al. (1999). Nuclear accumulation of truncated atrophin-1 fragments in a transgenic mouse model of DRPLA. *Neuron* **24**, 275-286.

Strutt, D. I. (2001). Asymmetric localization of frizzled and the establishment of cell polarity in the Drosophila wing. *Mol. Cell* **7**, 367-375.

Strutt, D., Johnson, R., Cooper, K. and Bray, S. (2002). Asymetric localization of Frizzled and the determination of Notch-dependent cell fate in the Drosophila eye. *Curr Biol.* **12**, 813-824.

Tomlinson, A. and Struhl, G. (1999). Decoding vectorial information from a gradient: sequential roles of the receptors Frizzled and Notch in establishing planar polarity in the Drosophila eye. *Development* **126**, 5725-5738.

Tree, D., Schulman, J., Rousset, R., Scott, M., Gubb, D. and Axelrod, J. D. (2002). Prickle mediates feedback amplification to generate asymmetric planar cell polarity signaling. *Cell* **109**, 371-381.

Usui, T., Shima, Y., Shimada, Y., Hirano, S., Burgess, R. W., Schwarz, T. L., Takeichi, M. and Uemura, T. (1999). Flamingo, a seven-pass transmembrane cadherin, regulates planar cell polarity under the control of Frizzled. *Cell* **98**, 585-595.

Villano, J. L. and Katz, F. N. (1995). four-jointed is required for intermediate growth in the proximal-distal axis in Drosophila. *Development* **121**, 2767-2777.

Wolff, T. and Ready, D. (1993). Pattern formation in the Drosophila retina. In *The Development of* Drosophila melanogaster, pp. 1277-1325. Cold Sping Harbor, NY: Cold Sping Harbor Laboratory Press.

Wood, J. D., Nucifora, F. C., Jr, Duan, K., Zhang, C., Wang, J., Kim, Y., Schilling, G., Sacchi, N., Liu, J. M. and Ross, C. A. (2000). Atrophin-1, the dentato-rubral and pallido-luysian atrophy gene product, interacts with ETO/MTG8 in the nuclear matrix and represses transcription. *J. Cell Biol.* **150**, 939-948.

Yang, C., Axelrod, J. D. and Simon, M. A. (2002). Regulation of Frizzled by Fat-like cadherins during planar polarity signaling in the Drosophila compound eye. *Cell* **108**, 675-688.

Yang, C. H., Simon, M. A. and McNeill, H. (1999). mirror controls planar polarity and equator formation through repression of fringe expression and through control of cell affinities. *Development* **126**, 5857-5866.

Zeidler, M. P., Perrimon, N. and Strutt, D. I. (1999). The four-jointed gene is required in the Drosophila eye for ommatidial polarity specification. *Curr. Biol.* **9**, 1363-1372.

Zeidler, M. P., Perrimon, N. and Strutt, D. I. (2000). Multiple roles for four-jointed in planar polarity and limb patterning. *Dev. Biol.* **228**, 181-196.

Zhang, S., Xu, L., Lee, J. and Xu, T. (2002). Drosophila atrophin homolog functions as a transcriptional corepressor in multiple developmental processes. *Cell* **108**, 45-56.

Zheng, L., Zhang, J. and Carthew, R. W. (1995). frizzled regulates mirror-symmetric pattern formation in the Drosophila eye. *Development* **121**, 3045-3055.